ELSEVIER

Surface Science 361/362 (1996) 525–528

surface science

Magnetotransport in wide parabolic PbTe quantum wells

J. Oswald [a,*], G. Heigl [a], M. Pippan [a], G. Span [a], T. Stellberger [a], D.K. Maude [b], J.C. Portal [b]

[a] *Institut für Physik, Montanuniversität Leoben, Franz Josef Strasse 18, A-8700 Leoben, Austria*
[b] *High Magnetic Field Laboratory, CNRS, 25 Avenue des Martyrs, BP 166 Grenoble, France*

Received 21 June 1995; accepted for publication 31 August 1995

Abstract

The 3D and 2D behaviour of wide parabolic PbTe single quantum wells, which consist of PbTe p–n–p structures, are studied theoretically and experimentally. A simple model combines the 2D sub-band levels and the 3D Landau levels in order to calculate the density of states in a magnetic field perpendicular to the 2D plane. It is shown that at a channel width of about 300 nm, one can expect to observe 3D and 2D behaviour at the same time. Magnetotransport experiments in selectively contacted Hall bar samples are performed at temperatures down to $T=50$ mK, and at magnetic fields up to $B=17$ T.

Keywords: Doping superlattices; Electrical transport; Electrical transport measurements; Lead telluride; Quantum effects; Quantum wells

1. Introduction

Wide parabolic quantum wells (WPQWs) are of particular interest because of the intermediate dimensionality of 2D and 3D physics. During the past few years, much effort in fabricating, investigating and modelling [1–3] of $Al_xGa_{1-x}As$ WPQWs has been made. The realization of wide quantum wells with a flat potential in the electron channel requires a parabolic bare potential which is difficult to obtain by MBE growth in quantum well systems. WPQWs can be made much more easily using the nipi concept [4].

PbTe is a narrow-gap semiconductor with both the conduction and the valence band extrema located at the L points of the Brillouin zone. The effective mass ellipsoids are oriented along the four $<111>$ directions and have a mass anisotropy of about a factor of 10. With respect to the growth direction, there are two different effective masses for both the sub-band quantization and the Landau level splitting. Therefore there are two sets of sub-bands and two sets of Landau levels for a magnetic field perpendicular to the 2D plane.

The PbTe layer systems are grown on $<111>$ BaF_2 substrates by hot wall epitaxy (HWE). The p-layers of the p–n–p structures are designed to be non-depleted in order to screen the embedded n-channel from any influence from surface and interface states [4]. Selective contacts to the embedded n-channel are realised [5] in order to perform magnetotransport experiments. The mobility in this selectively contacted structures is in the order of 1×10^5–1×10^6 $cm^2V\cdot s^1$ at lowest temperatures. The large dielectric constant ($\epsilon=$

* Corresponding author. Fax: +43 3842 402 760; e-mail: oswald@unileoben.ac.at.

PII S0039-6028(96)00461-X

500–1000) leads to wide quasi-parabolic potential wells with a typical sub-band separation ranging from 1 to 3 meV.

2. Model

The sub-band energies are calculated self-consistently by a numerical solution of the Schrödinger equation within the effective mass approximation at zero magnetic field. The Landau levels (LLs) are obtained from a 3D calculation according to Refs.[6,7]. The energy level system $E_{ij}(B)$ consists of all LLs $E_j(B)$ sitting on all sub-band levels E_i according to a "rigid potential model". Since in wide quantum wells the Landau level separation is much higher than the sub-band splitting, the LLs can be considered to be split by the sub-band quantization. The calculation of the density of states (DOS) is done by a superposition of the individual Landau peaks with a broadening factor b. The broadening function in this approximation is assumed to be Gaussian. The DOS as a function of energy E and magnetic field B then reads as follows [8]

$$\mathrm{DOS}(E,B)=\frac{q_e B}{h}\sum_{i,j}\frac{1}{b\sqrt{\pi}}\times\left(\mathrm{e}^{-\frac{(E-E_j^1(B))^2}{b^2}}+3\,\mathrm{e}^{-\frac{(E-E_j^0(B))^2}{b^2}}\right),$$

where 1 denotes the longitudinal and o the oblique valleys, i denotes the sub-band level index and j the Landau level index. The numerical factor 3 in the second term in brackets accounts for the three-fold degeneracy of the oblique valleys.

Fig. 1 shows the result of the model calculation of a WPQW with parameters according to the sample used in the experiment. For this sample, the carrier sheet density is $n_{2D}=9.8\times10^{12}\ \mathrm{cm}^{-2}$ and the background doping level in the electron channel is $N_D=3\times10^{17}\ \mathrm{cm}^{-3}$, resulting in an effective electron channel width of $d_n=330$ nm. The shape of the screened potential is a mixture of a square potential (flat region in the middle of the channel) and a parabolic potential. Therefore the sub-band splitting is very small for the lower sub-bands, and it increases with the sub-band index. Finally, at high sub-band energies it approaches the constant sub-band spacing according to the parabolic bare potential. Consequently the associated Landau levels (of same Landau index) of the lower sub-bands cause an overall enhancement of the density of states near the sub-band ground state. The energy of the sub-band ground state is nearly identical to the position of the associated 3D LL (LL of a 3D sample). At higher sub-band energies the sub-band levels are separated more and more, and therefore a modulation of the DOS by the sub-band structure is more and more pronounced. For magnetotransport experiments the 2D model predicts an overall enhancement of the DOS at the energy position of the 3D LLs and therefore also bulk-like Shubnikov–de Haas (SdH) oscillations of the magnetoresistance can be expected. At higher sub-band energies, which means the energy range between the 3D LLs, a modulation of the DOS due to the sub-band structure of the oblique valleys can be expected. The LLs of the sub-band ground states are plotted in Fig. 1a. The LL energies at $B=8$ T are marked by arrows guiding from Fig. 1a to Fig. 1b, in which the total DOS at $B=8$ T is plotted. The contribution of the longitudinal valley to the DOS is more or less a uniform background because of the much smaller sub-band separation. The contribution of the longitudinal valley is plotted by a dashed line. Due to the lattice mismatch between BaF_2 and PbTe, a strain-induced energy shift between the longitudinal and the oblique valleys of 5 meV is included in the calculation. This value depends strongly on the sample history and is consistent with the value of Ref. [9].

3. Experiments

The sample parameters in the experiment are those used for the model calculation in Section 2. The shape of the sample is a conventional Hall bar of $w=90\ \mu$m width. The experiments were performed in an 11 T superconducting magnet at pumped ^{4}He temperature and in a 17 T superconducting magnet with a dilution refrigerator. A conventional lock-in technique using an AC cur-

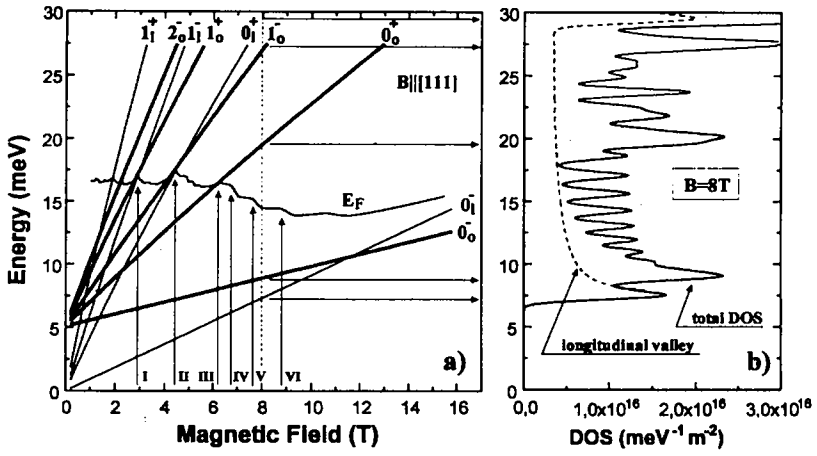

Fig. 1. (a) Landau levels of the sub-band ground states and Fermi energy versus magnetic field. Numbers denote the LL index, l and o denote the longitudinal and the oblique effective mass ellipsoids, + and − denote the spin orientation. (b) Density of states at $B=$ 8 T. Dashed line: contribution of the longitudinal valley to the total DOS.

rent of 10 nA at $T=50$ mK and 100 nA at $T=2.2$ K was used. The results are shown in Fig. 2. SdH oscillations according to the 3D parameters of the sample dominate the magnetotransport experiments and no additional structure in the data at $T=2.2$ K is found. At lower temperatures structures in addition to that found at $T=2.2$ K appear in the upper field range. These smooth structures are covered by strong fluctuations which are perfectly reproducible. The position of the main features are labelled I–VI and should compare with the calculation in Fig. 1. Three different sweeps at $T=50$ mK are shown in order to demonstrate the reproducibility of the data. For better visibility, all plots apart from the thick solid trace are shifted vertically by a small amount.

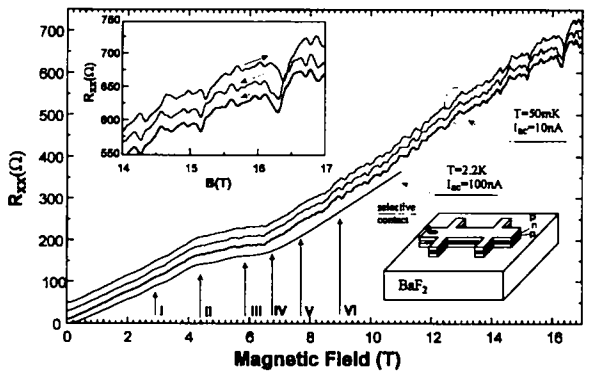

Fig. 2. Magnetoresistance data. The labelled arrows indicate the position of the main features, which should be compared with Fig. 1. Upper insert: magnification of the higher field range. The arrows indicate the sweep direction. Lower insert: scheme of the sample configuration with one representative selective contact.

4. Discussion and concluding remarks

The modulation of the DOS at the Fermi level results from changes of the individual filling factors of the different sub-band systems involved. The carrier distribution between the different sub-band systems changes with the magnetic field. Since only the total filling factor is periodic in $1/B$, a plot of the data over $1/B$ cannot be used to check the periodicity. At 2.2 K only a structure at I, II and III is visible, while structures at IV, V and VI appear at the lowest temperatures only. From comparison with the calculation I, II and III can be attributed to 3D SdH oscillations, and IV, V and VI can be attributed to the 2D sub-band quantization. The appearance of strong fluctuations in parallel to the appearance of the 2D features is an indication of the formation of edge states by the oblique valleys, while at the same time the longitudinal valley still enables bulk conduction. As an example, an intermediate regime between quantum edge conduction and bulk trans-

port was investigated by Geim et al. in n^+-GaAs epilayers [10], and it was shown that the edge states play an important role in carrying the current to classically inaccessible regions. In contrast to the GaAs system, the edge-state conduction and the bulk conduction result from electrons in different valleys. Therefore a coexistence of perfect edge state conduction and bulk conduction is possible, and new effects resulting from the interplay of these two electron systems can be expected. The observed fluctuations are the subject of further investigations, and will be published elsewhere.

Acknowledgements

Financial support by Fonds zur Förderung der wissenschaftlichen Forschung (FWF) Vienna (Project No. P10510-NAW) and by Steiermärkischer Wissenschafts- und Forschungslandesfonds is acknowledged.

References

[1] A.J. Rimberg and R.M. Westervelt, Phys. Rev. B 40 (1989) 3970.
[2] C.E. Hembre, B.A. Mason, J.T. Kwiatkowski and J.E. Furneaux, Phys. Rev. B 50 (1994) 15197.
[3] M. Shayegan, T. Sajoto, M. Santos and C. Silvestre, Appl. Phys. Lett. 53 (1988) 791.
[4] J. Oswald, B. Tranta, M. Pippan and G.Bauer, Opt. Quantum Electron. 22 (1990) 243.
[5] J. Oswald and M. Pippan, Semicond. Sci. Technol. 8 (1993) 435.
[6] H. Burkhard, G. Bauer and W. Zawadzki, Phys. Rev. B 19 (1979) 5149.
[7] J. Oswald, P. Pichler, B.B. Goldberg and G. Bauer, Phys. Rev. B 49 (1994) 17029.
[8] J. Oswald, M. Pippan, G. Heigl, G. Span and T. Stellberger, in Proc. 7th Int. Conf. on Narrow Gap Semiconductors, Santa Fe, NM, 1995, Inst. Phys. Conf. Ser. 144 (1995) 155.
[9] J. Oswald, B.B. Goldberg, G. Bauer and P.J. Stiles, Phys. Rev. B 40 (1989) 3032.
[10] A.K. Geim, P.C. Main, P.H. Beton, P. Streda and L. Eaves, Phys. Rev. Lett. 67 (1991) 3014.